Surface Science 87 (1979) 101–111

CLASSICAL TRAJECTORY CALCULATIONS OF THE ENERGY DISTRIBUTION OF EJECTED ATOMS FROM ION BOMBARDED SINGLE CRYSTALS

B.J. GARRISON * and N. WINOGRAD *

Department of Chemistry, Pennsylvania State University, University Park, Pennsylvania 16802, USA

and

D.E. HARRISON, Jr.

Department of Physics and Chemistry, Naval Postgraduate School, Monterey, California 93940, USA

Received 28 February 1979

The energy distribution of particles ejected from single crystal surfaces has been calculated using classical dynamics. The model utilizes a microcrystallite of 4 layers with ~60 atoms/layer which is bombarded by 600 eV Ar^+ at normal incidence. Calculations have been performed for the clean (100) face of copper as well as for copper with oxygen placed in various coverages and site geometries. The energy distributions for Cu, O, Cu_2, CuO and Cu_3 are reported for this system. The distribution for clean Cu exhibits structure which is shown to arise from preferred ejection mechanisms in the crystal. For oxygen adsorbates, the effect of the oxygen binding energy on the peak in the energy distribution of the ejected oxygen atoms is examined by arbitrarily varying the well-depth of the Cu–O pair potential. In general, higher values of the binding energy produce a maximum in the curve at higher energies and also produce a broader energy distribution. The O_2 and Cu_2 dimer distributions are found to peak at approximately the same energy as the O and Cu curves when compared on a kinetic energy/particle basis, although their widths are considerably smaller. Finally, we predict that the CuO energy distribution should be wider than either the Cu_2 or O_2 distributions since it results from the convolution of the Cu and O distributions which are quite different.

1. Introduction

A theoretical description of the interaction of kilovolt ion beams with solid surfaces has recently evolved from classical dynamical calculations of the momentum deposition process [1–6]. This description has been useful in elucidating the factors that influence many of the experimental observables such as relative monomer yields [2], angular distributions [5], relative multimer yields [1] and multimer formation mechanisms [4]. The model has also been adapted to include atomic [3]

* Work performed at Purdue University, West Lafayette, Indiana 47907, USA.

and molecular adsorbates [6] placed in specific coverages and site geometries. A general conclusion from these studies is that the crystal structure of the substrate and the placement of the adsorbates are important factors in determining the mechanism of momentum dissipation. The appropriate application of ion beams to the determination of surface crystal structure and morphology seems feasible.

The energy distribution of particles ejected from ion-bombarded surfaces has been measured for many systems. The relationship between the shape of the energy distribution curves and the nature of the crystalline surface has not been fully elucidated. Jackson [7] has noted that the energy of the ejected particles is anisotropic and dependent on crystal structure. The relationship would appear to be a fairly complex one, since a multitude of ejection mechanisms are known to contribute to the ejection of particles. The interpretation of the shape of the energy distribution curve, then, is largely speculative.

To our knowledge only two previous workers have theoretically discussed the energy distributions of the low energy (<10 eV) ejected neutral particles. Thompson employed a random cascade of binary collisions with an isotropic velocity distribution inside the solid [8,9]. From this model he predicted that the peak of the distribution should appear at $E_p \approx E_{b/2}$ where E_b is the binding energy of the solid. His equations also predict that the full width at half maximum (FWHM) of the peak is $\sim 1.9\ E_b$. From our calculations we find that the positions of the maxima are in semi-quantitative agreement with Thompson's model but that the width of the distributions differ significantly from his predictions. In addition, there are strong anisotropy effects in the energy distributions which are not included in any isotropically-based model.

For the case of multimer formation Können, Tip and DeVries [10] have derived a theoretical expression for dimer energy distributions by a convolution of Thompson's equation for monomers. An assumption in their model is that dimers only form from nearest neighbor surface atoms. This assumption for clean metals is in conflict with recent calculations aimed at modeling cluster ejection which show that dimers originate from a localized region on the surface but that only ~30% are nearest neighbors [1].

In this paper we present results from a full molecular dynamics calculation for an ion-bombarded solid in hopes of elucidating the factors that influence the shape of both the monomer and multimer energy distributions of the ejected particles. We have examined single crystals, primarily the (100) face of an fcc crystal, and have completed the first calculations for energy distributions for an ordered adsorbate overlayer using oxygen chemisorbed on the (100) face of a Cu crystal as a model system.

2. Description of the calculation

To determine the energy distributions of particles ejected from a solid due to ion bombardment, we determine the positions and momenta of all particles in and on

the solid as a function of time. The solid is modeled by a microcrystallite of 4 layers with approximately 60 atoms/layer (total of ~240 atoms). For some of the calculations we have also placed adsorbates on the surface of the crystallite. For our model calculations the metal is assumed to be a copper fcc crystal with an oxygen adsorbate, with most of the calculations being done on the (100) face. For these calculations the primary ion is Ar^+ which strikes the crystal at normal incidence with 600 eV of kinetic energy. The subsequent motion of all particles is determined by integrating Hamilton's equations. A complete description of the calculation and of the interaction potentials has been given elsewhere [2,3]. After the collision cascade has been terminated the final positions and momenta are analyzed for multimer formation [1,3].

Of particular interest in this study is to characterize the influence of the binding energy, E_b, on the shape of the energy distribution curve. In this work we define E_b to be the sum of the pairwise interactions of an atom with the rest of the atoms while in its equilibrium position [3]. The value for E_b can be varied by adjusting the strength of the attraction in the pairwise additive interaction.

The shape of energy distribution curves for all size clusters is similar to that shown in fig. 1. The probability of particle ejection increases with increasing energy, reaches a maximum and for monomers decreases as approximately $E^{-1.5}$.

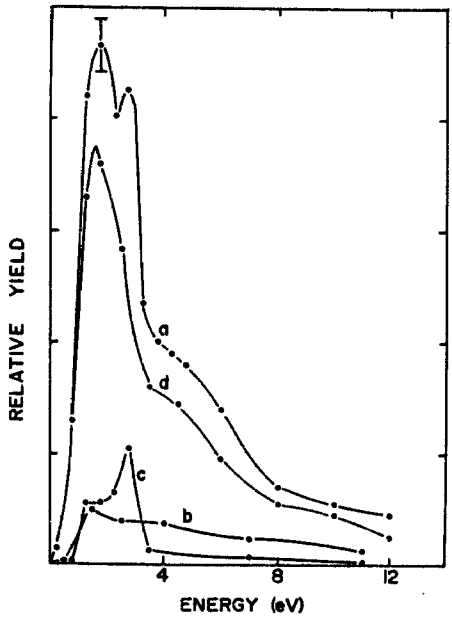

Fig. 1. Energy distribution of Cu atoms from the clean (100) face: (a) is drawn for all Cu atoms; (b) is for atoms 1–5 of fig. 2, (c) is for atoms 6–9 of fig. 2 while (d) is drawn for the remaining atoms not included in (b) and (c).

The quantity that Thompson [8] has associated with the peak position and width is the binding energy E_b of an atom to the solid surface. By making an approximation he predicts the peak to occur at $E_{b/2}$. By making the same approximation the full width at half maximum should be $\sim 1.9\, E_b$.

For a typical system we compute 50–100 trajectories initiated over a zone of irreducible symmetry located in the center of the crystal surface. For determination of yields and angular distributions, the calculation of larger numbers of impact points does not significantly improve the results. For determination of energy distributions, however, smooth curves with resolution of ~0.5 eV require many times more calculations. For the limited data presently available, it is not possible to distinguish the energy distributions of, for example, ejected oxygen atoms in different sites but with the same E_b. Thus, we have occasionally added several runs together to achieve better statistics. This procedure is specifically noted when it has been applied.

3. Results and discussion

3.1. Clean surfaces

The shape of the energy distribution curve for atoms ejected from clean surfaces is similar to that shown in fig. 1a. In general, the probability of particle ejection increases with increasing energy, reaches a maximum and decreases as approximately $E^{-1.5}$. More detailed experiments, however, have revealed the presence of structure superimposed on this general shape [9,11]. Thompson has proposed that at least some of this structure is a manifestation of focussed collision sequences in the solid [8,9]. Of particular interest is that when our calculated distributions are analyzed under higher resolution conditions than previously reported [1], additional peaks are clearly apparent. In fig. 1a, note that there is considerable structure including a peak at ~2.7 eV and a shoulder at ~5 eV. The shoulder(s) on the high energy side of the peak are also seen experimentally [9,11]. Our analysis of the many individual trajectories clearly shows that the structure is not necessarily due to focussed collision sequences, rather that there are distinct, preferred mechanisms that cause given atoms to eject. Each atom thus has a characteristic energy distribution, which does not necessarily match the total distribution. Since the observed curve is then a linear combination of each atom's distribution, it is quite feasible that there be structure.

From a careful analysis of the dynamic motion of atoms during each impact, it is possible to correlate specific ejection mechanisms with localized regions of the impact zone. In addition, we can compute the energy distribution curve for these specific processes. For example, the energy distribution of atoms labeled 1–5 of fig. 2, is given in fig. 1, curve b. Of these five atoms, numbers 2 and 4 eject the most frequently and primarily when the Ar^+ impacts near the hypotenuse of the triangu-

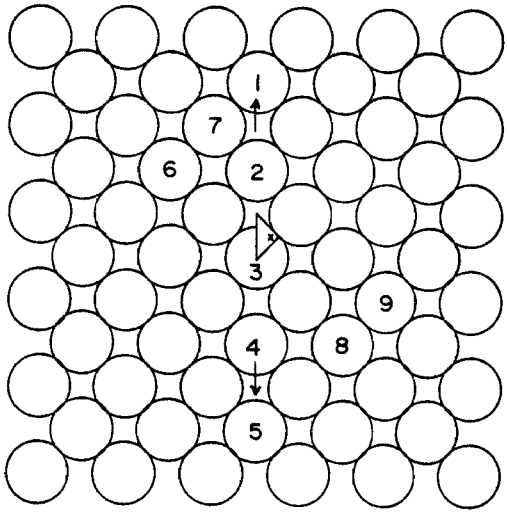

Fig. 2. Clean Cu(100) surface. The numbers are used to identify particular atoms (see text). The impact zone is denoted by the triangle.

lar impact zone. Atom 2 ejects by the Ar^+ reflecting from the second layer and hitting it from behind. As the Ar^+ initially penetrates the surface, it pushes atom 3 which also reflects from the second layer ejecting atom 4. Atoms 2 and 4 generally eject with a considerable amount of kinetic energy and in a direction as indicated by the arrows in fig. 2. Accordingly, the energy distribution of atoms 1–5 is very flat with virtually no peak and a long high energy tail.

Another example illustrating the correspondence between specific impact regions and preferred ejection mechanisms is also shown in fig. 2. When the Ar^+ ion strikes the region denoted by the X, atoms 6–9 are found to eject frequently. Note that this region has nearly four fold symmetry which results in the ejection of 4 symmetrically equivalent atoms. Their energy distribution is shown in curve c of fig. 1. This curve has a peak at the same energy as the second peak in the total distribution. The energy distribution of the remainder of the atoms is given by curve d. There are undoubtedly more mechanisms that could be unfolded from the complete curves. The main point is that the ejection process is not random and not isotropic.

It is interesting to analyze this concept a little further in reference to the angular distribution of the ejected atoms. We have recently shown that the anisotropic angular distributions are considerably enhanced if only particles with kinetic energy greater than 20 eV are collected [5]. This is because the "spot" or peak in intensity of the angular distribution is due mainly to atoms 1–5 of fig. 2, which are primarily high energy particles. In table 1, we show that atoms 1–5 comprise only 28% of the total number of monomers ejected, yet they contribute to 53% of the high energy

Table 1
Distribution of ejected energies of specific atoms on Cu(100)

	Atoms	
	1–5 [a]	Rest
Fraction of total monomers	0.28	0.72
Fraction of monomers with energy in the range:		
0–20 eV	0.18	0.82
>20 eV	0.53	0.47

[a] Labeling is denoted in fig. 2.

distribution. It is these highly energetic particles which generally reflect the crystal structure and give rise to the sharp peaks in the angular distributions.

The presence of the variety of ejection mechanisms which contribute to different regimes of the energy distribution illustrate that the concept of a surface binding energy is somewhat vague. The atoms that are ejected early in the collision cascade, when the surface is still intact, may truly experience a unique characteristic binding energy. These particles, however, generally eject with large kinetic energy and do not contribute to the peak in the energy distribution curve. The low energy atoms that do contribute to the peak and which are thought to be most affected by the surface binding energy, generally leave late in the collision sequence when the surface has been considerably disrupted and a characteristic binding energy is not well defined.

3.2. Oxygen covered metal surfaces

The classical dynamical model is also applicable to describing the ejection mechanisms which occur on chemically reacted single crystal surfaces. This situation is of particular interest to interpreting experiments aimed toward elucidating the structure of these systems. A few experimental energy distribution curves have been published for O_2 on Mo [12] although the results have not been interpreted. We have examined oxygen atoms adsorbed on the three low index faces of Cu with the oxygen placed in several site positions and in varying coverages. Of particular interest is that the relationship between E_b and the shape of the ejected oxygen atom energy distribution can be probed in detail by arbitrarily adjusting the strength of the attraction in the Cu–O pair potential.

In fig. 3, we show the calculated energy distribution for oxygen adsorbates on a Cu(100) crystal for $E_b = 0.75$ eV (curve a) and $E_b = 2.00$ eV (curve b). The results represent the composite of runs completed on several different adsorbate positions to improve statistical reliability. This averaging may suppress some of the fine-struc-

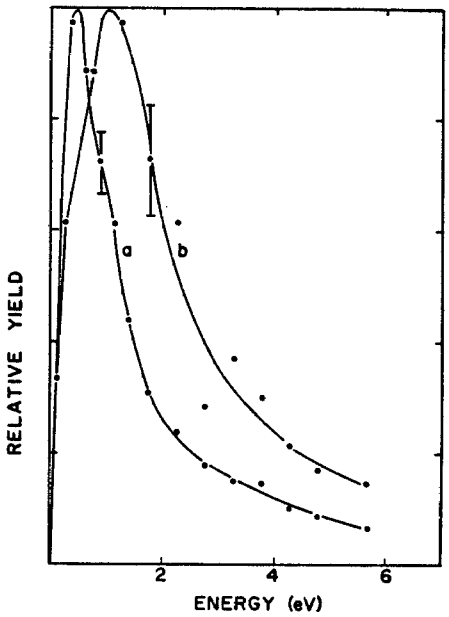

Fig. 3. Energy distribution of ejected oxygen atoms: (a) is calculated for E_b = 0.75 eV and (b) is calculated for E_b = 2.0 eV.

ture in the curves, but is a necessary procedure to provide enough ejected particles for energy resolution of 0.25 eV.

The results shown in fig. 3 are in qualitative agreement with Thompson's theory for the energy distribution, a surprising result considering the approximations in his model. The observed peak energies, E_p of ~0.5 and ~1.0 eV for the two cases are close to this predicted value of $\frac{1}{2} E_b$. The FWHM of 1.1 and 2.2 eV are in worse agreement, however, with Thompson's predicted values of 1.4 and 3.8 eV. This variation could arise since to approximate the peak position and width, an integral expression was assumed to be a constant value [8]. We believe, however, that this variation is due to the neglect of anisotropic effects illustrated in section 3.1. It is of interest to compare the energy distribution of clean Cu(100), fig. 1a, to that of oxygen adsorbed on Cu(100), fig. 3. In general, the oxygen distributions are more sharply peaked at lower energies than the Cu distributions, since the binding energies used for the oxygen are less than for the copper.

3.3. Energy distribution of the clusters

As a result of our model, we have proposed that the observed clusters ejected from clean and oxygen covered metal surfaces form from atomic collisions above the solid and do not necessarily consist of atoms that were contiguous on the sur-

face. The criterion for cluster stability is that the total energy of the cluster, $E_{\text{tot}}^{\text{cluster}}$ be less than zero where $E_{\text{tot}}^{\text{cluster}}$ is defined

$$E_{\text{tot}}^{\text{cluster}} = T_{\text{R}}^{\text{cluster}} + \sum_{i=1}^{n-1} \sum_{j>i}^{n} V_{ij} .$$

In this definition $T_{\text{R}}^{\text{cluster}}$ is the relative kinetic energy of the cluster atoms, V_{ij} is the potential energy between any pair of atoms i and j and n is the number of atoms in the cluster. A consequence of this definition is that the peak position in the energy distribution curve should reflect the binding energy of atomic constituents and not of the cluster. Since the cluster has no special molecular identity when it is in the solid, it is difficult to even define a binding energy of the cluster to the solid.

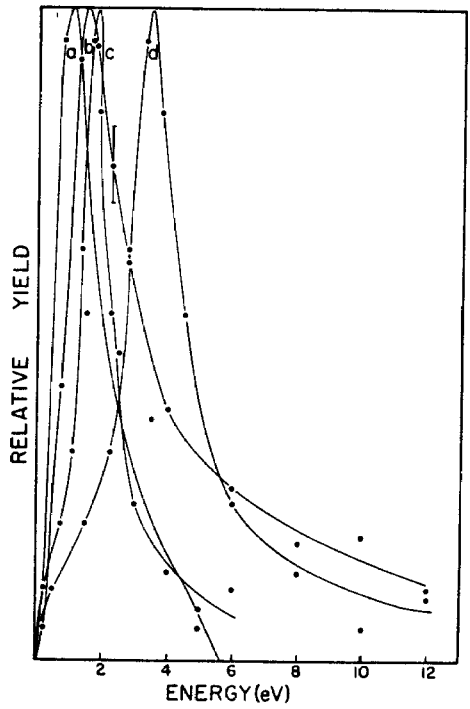

Fig. 4. Cu, Cu_2 and Cu_3 energy distributions: (a) Cu_2 versus $T_{\text{com}}/2$; (b) Cu; (c) Cu_3 versus $T_{\text{com}}/3$; (d) Cu_2 versus T_{com}. The Cu and Cu_2 distributions are the combination of several runs with oxygens adsorbed with E_b = 0.75 eV. The Cu_3 distribution is from the Cu(111) surface with oxygen adsorbed in various sites since the (111) face is the only one that yields a significant number of trimers. Due to the large uncertainty in the points in (a), (c) and (d), we have drawn lines that are only a guide to the eye and have no physical significance.

Based on this definition of a cluster we have plotted the energy distributions for copper dimers, monomers and trimers in fig. 4, curves a–c. Note that as the size of the cluster increases, that the FWHM decreases. This correlation is in qualitative agreement with experiments on W_n^+ [13], Si_n^+ [14] and K_2 [10] clusters and results from the fact that when the constituent atoms possess low kinetic energies, any pair of atoms have a higher probability of having a lower value of T_R. This condition enhances the probability that $E^{tot}_{cluster}$ will be less than zero. The multimer distributions essentially terminate around 6–10 eV/particle, although a few dimers with 10–20 eV/particle are found. This observation is in contrast to the distributions for monomers which have long tails extending to about 200 eV [2].

The distributions presented in curves a–c of fig. 4 are plotted versus the center of mass kinetic energy, T_{com}/particle. Although T_{com}/particle is not a meaningful experimental quantity, it does represent typical energies of the atoms that have a propensity to form clusters. In curve d of fig. 4, we show the dimer distribution plotted versus the total T_{com}. When the distributions are graphed versus T_{com}/particle, the monomer, dimer and trimer distributions peak at essentially the same

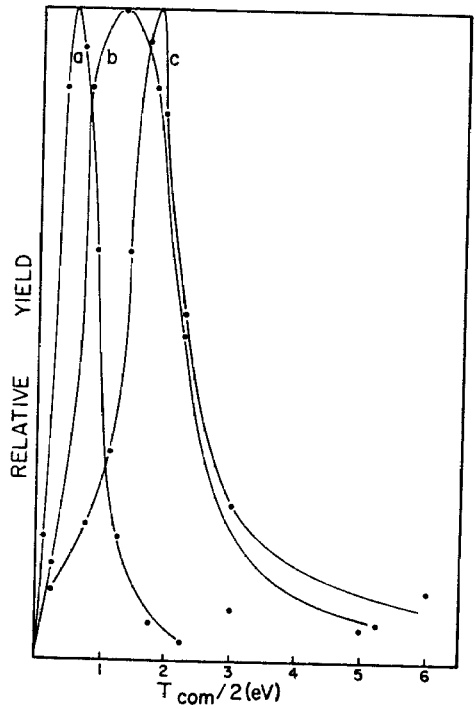

Fig. 5. Cu_2, O_2 and CuO energy distributions: (a) O_2; (b) CuO; (c) Cu_2. Data for several site positions and coverages of O atoms on Cu(100) with an oxygen binding energy of 0.75 eV have been added together to yield sufficient statistics to obtain smooth curves.

energy. The error bars for the dimer and trimer distributions are about 3 and 5 times, respectively, the error bars on the monomer distribution. It is therefore difficult to precisely determine the peak positions and widths of the multimer curves. In general, however, we would expect E_p for the homonuclear clusters to appear at the same energy as the monomers when plotted versus T_{com}/particle, and not when plotted versus the total T_{com}.

A simple description of the heteronuclear dimers, e.g., CuO, are somewhat more complicated to understand than the homonuclear systems. As is evident from figs. 1a and 3b, the FWHM of the Cu distribution is considerably larger than that of the O distribution for a binding energy of 0.75 eV, Since the dimer distribution is essentially a convolution of two distinct monomer energy distributions, we expect, as shown in fig. 5b, that the CuO distribution will have a much larger FWHM than either O_2 or Cu_2 (figs. 5a and 5c). To our knowledge, no experimental data for neutral dimers is available to test this prediction, although Dawson has found that MoO^+ has a broader energy distribution than Mo_2^+ [12].

4. Conclusions

Using a full dynamical model we have calculated the energy distributions of monomers, dimers, and trimers ejected from ion bombarded single crystals. The energy distribution curves have considerable structure, which arises because different atoms eject via different mechanisms each having a characteristic energy distribution curve. Thus the total curve is a linear combination of individual atom distributions. The peak position and width reflect the binding energy E_b of the atom to the solid. However, the statistics in the calculation are not good enough to ascertain a precise dependence. We question the significance of this correlation since the binding energy is not a well-defined quantity. Most of the atoms eject late in the collision cascade after considerable atomic motion has destroyed most of the surface structure. Thus the peak position should not precisely reflect a binding energy of the undamaged crystal.

The O_2 and Cu_2 dimer distributions peak at approximately the same energy as the O and Cu curves when plotted on a kinetic energy per particle basis. In general, the dimer distributions are narrower as they are basically convolutions of the monomer distributions and do not exhibit a high energy tail. For a dimer (or any cluster) to form the constituent particles must be moving with low relative kinetic energy so that they can experience binding interactions. This condition becomes more unlikely as the energy of the particles increases. The CuO energy distribution curve however is wider than either the Cu_2 or O_2 distributions since it results from the convolution of two very different curves.

The general features of the classical dynamical predictions for the energy distribution of the ejected particles are not in complete disagreement with several simplified currently accepted analytic models. On the other hand, these equations cannot

be extended to elucidate anisotropic ejection mechanisms from single crystals, the origin of the observed structure in the energy distributions or the expected shape of the cluster distributions. We further believe that only by utilizing the classical dynamics approach can detailed agreement between experiment and theory be expected.

Acknowledgements

This research was partially supported by grants from the National Science Foundation (CHE78-08728 and DMR/MRL 77-23793) and the Air Force Office of Scientific Research (AF76-2974). Portions of the computations were supported by the Foundation Research Program of the Naval Postgraduate School with funds provided by the Chief of Naval Research and by the National Resource for Computation in Chemistry under a grant from the National Science Foundation and the US Department of Energy (Contract No. W-7405-ENG-48).

References

[1] N. Winograd, D.E. Harrison, Jr. and B.J. Garrison, Surface Sci. 78 (1978) 467.
[2] D.E. Harrison, Jr., P.W. Kelly, B.J. Garrison and N. Winograd, Surface Sci. 76 (1978) 311.
[3] B.J. Garrison, N. Winograd and D.E. Harrison, Jr., Phys. Rev. B18 (1978) 6000.
[4] B.J. Garrison, N. Winograd and D.E. Harrison, Jr., J. Chem. Phys. 69 (1978) 1440.
[5] N. Winograd, B.J. Garrison, and D.E. Harrison, Jr., Phys. Rev. Letters 41 (1978) 1120.
[6] N. Winograd, B.J. Garrison and D.E. Harrison, Jr., Phys. Rev. B, submitted.
[7] D.P. Jackson, Can. J. Phys. 53 (1975) 1513.
[8] M.W. Thompson, Phil. Mag. 18 (1968) 377.
[9] B.W. Farmery and M.W. Thompson, Phil. Mag. 18 (1968) 415.
[10] G.P. Können, A. Tip and A.E. DeVries, Radiation Effects 21 (1974) 269.
[11] See for example, P. Hucks, G. Stocklin, E. Vietgke and K. Vegelbruch, J. Nucl. Mater. 76 (1978) 136.
[12] P.H. Dawson, Phys. Rev. B15 (1977) 5522.
[13] G. Staudenmaier, Radiation Effects 13 (1972) 87.
[14] K. Wittmaack, Phys. Letters 69A (1979) 322.